REVIEW ARTICLE

Magnetic resonance imaging of bone marrow in oncology, Part 1

Sinchun Hwang · David M. Panicek

Abstract Magnetic resonance imaging plays an integral role in the detection and characterization of marrow lesions, planning for biopsy or surgery, and post-treatment follow-up. To evaluate findings in bone marrow on MR imaging, it is essential to understand the normal composition and distribution of bone marrow and the changes in marrow that occur with age, as well as the basis for the MR signals from marrow and the factors that affect those signals. The normal distribution of red and yellow marrow in the skeleton changes with age in a predictable sequence. Important factors that affect MR signals and allow detection of marrow lesions include alterations in fat–water distribution, destruction of bony trabeculae, and contrast enhancement. This two-part article reviews and illustrates these issues, with an emphasis on the practical application of MR imaging to facilitate differentiation of normal marrow, tumor, and treatment-related marrow changes in oncology patients.

Keywords Magnetic resonance imaging · Marrow · Metastases · Tumor · Sarcoma · Treatment effects

S. Hwang · D. M. Panicek (✉)
Department of Radiology,
Memorial Sloan-Kettering Cancer Center,
1275 York Avenue,
New York, NY 10021, USA
e-mail: panicekd@mskcc.org

S. Hwang · D. M. Panicek
Weill Medical College of Cornell University,
New York, NY 10021, USA

Introduction

Bone marrow is one of the largest organs in the body after the osseous skeleton, skin, and body fat [1, 2], and is mainly composed of fat and water [1, 3]. Marrow can weigh up to 3 kg in an adult [2]. As such, at least some marrow is visible on nearly every CT and MR image, and can pose diagnostic challenges at each stage of a cancer patient's clinical course—from the initial detection of the tumor through staging and subsequent post-treatment evaluation, to surveillance for tumor recurrence. To a large extent, MRI is superior to other imaging modalities in evaluating bone marrow because it is remarkably sensitive in detecting lipid; therefore, MRI can be used to detect processes that alter the relative amounts of fat and water in bone marrow. In order to interpret the appearances of marrow seen on MRI and to distinguish normal from abnormal, it is important to understand the normal components and composition of bone marrow, which vary greatly with age and anatomic location within the skeleton [4–6]

Components and composition of normal bone marrow

The cellular components of bone marrow include stem cells, erythrocytes, myeloid cells, and megakaryocytes [2]. These cells, which are critical for maintaining oxygenation, immunity, and coagulation, reside around a network of cancellous bony trabeculae lined by fibrous tissue reticulum; the remaining marrow space is occupied by fat (Fig. 1).

On gross examination, bone marrow appears red (hematopoietic marrow) or yellow (fatty marrow) depending on its predominant components. Despite its unclear physiological role, fat is the major component of both yellow marrow and (to a lesser extent) red marrow. In the iliac crests of adults,
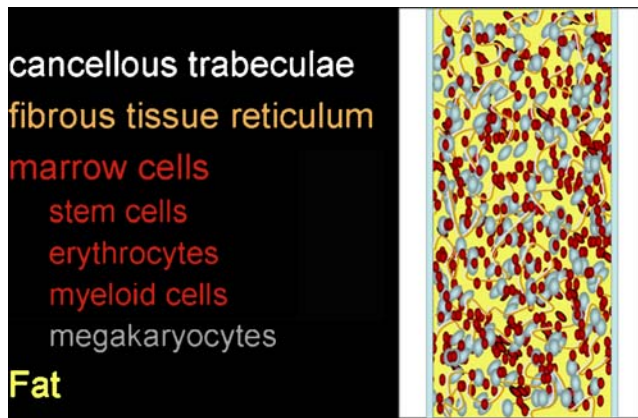
Fig. 1 Components of bone marrow. Schematic diagram of a cross-section of a diaphysis shows bone marrow as a network of bony trabeculae and fibrous reticulum surrounded by hematopoietic cells and fat

approximately 50–60% of marrow is hematopoietic [7]. The cellular composition of red marrow consists of 60% hematopoietic cells and 40% adipocytes; its chemical composition is 40–60% lipid, 30–40% water, and 10–20% proteins [1, 2]. In contrast, yellow marrow is nearly entirely composed of adipocytes (95%), with its chemical composition being 80% lipid, 15% water, and 5% protein [1].

Conversion of bone marrow

At birth, hematopoietic marrow is present throughout the entire skeleton, but various regions of hematopoietic marrow then start to convert to fatty marrow. The transition occurs over two decades in a predictable sequence, beginning in the periphery of the skeleton and extending in a symmetric, centripetal manner into the central skeleton (Fig. 2a) [1, 7]. Postnatally, marrow conversion starts in the terminal phalanges. Epiphyses and apophyses, when ossified, contain fatty marrow. In the first decade of life, a superimposed additional sequence of marrow conversion begins in the long bones, starting in the diaphyses and progressing toward the metaphyses (particularly the distal metaphysis; Fig. 2b). In the second decade, the long bone marrow becomes predominantly yellow except for residual regions of red marrow in the proximal metaphyses. In the late third decade, the bone marrow distribution achieves its mature state, with red marrow remaining throughout the axial skeleton (skull, spine, sternum, clavicles, scapulas, pelvis) and the humeral and femoral proximal metaphyses. From that point on, a gradual conversion of red marrow to yellow marrow occurs in the remainder of the skeleton, its speed dependent on patient gender and underlying medical conditions [1].

In normal adult marrow, yellow marrow may reconvert to red marrow in the event of a functional demand for increased

hematopoiesis. Benign conditions triggering reconversion include heavy smoking, long distance running, obesity, and middle age in women [8, 9]. Chronic disorders resulting in anemia (such as hemoglobinopathies and chronic infection) are also associated with diffuse red marrow hyperplasia [10]. Diffuse hematopoietic marrow hyperplasia may be difficult to distinguish from diffuse marrow disease on MRI [11].

The reconversion process proceeds in the exact reverse sequence from that of the initial conversion (Fig. 2): namely, from the central to the peripheral skeleton; and in the long bones, from the proximal metaphyses and then the distal metaphyses to the diaphyses [1]. Reconversion occurs more quickly in flat bones (such as the sternum, spine, and scapula) because they retain cellular marrow throughout life [1].

Factors affecting MR signal intensity of marrow

Vanel et al. [12, 13] have summarized three main factors that affect the signal intensity of bone marrow on MRI: the fat and water content of the marrow, the presence of bony
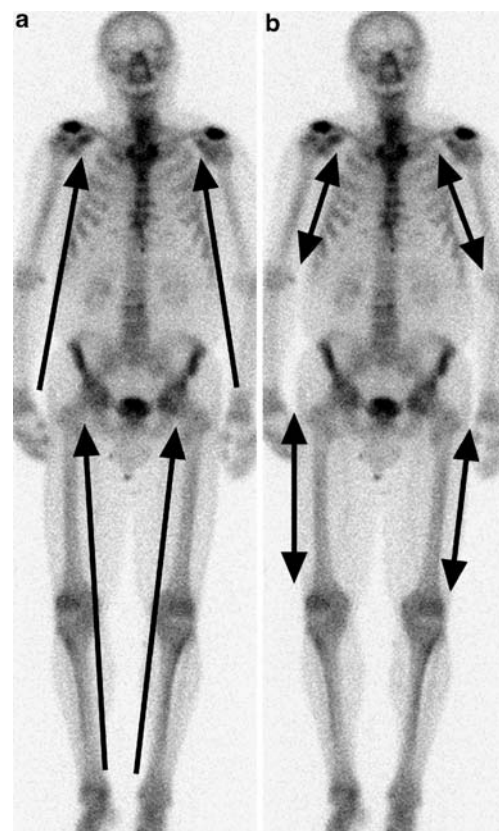
Fig. 2 Age-related conversion of bone marrow: two superimposed sequences (shown using bone scan for anatomic reference purposes only). **a** Red marrow converts to yellow marrow from the peripheral to the central skeleton (*arrows*). **b** Superimposed on that sequence, red marrow converts to yellow proceeding from diaphysis to metaphysis in long bones (*double-headed arrows*). Both of these sequences reverse during reconversion from yellow marrow to red marrow

trabeculae, and the use of contrast material. The MRI appearance of marrow is also dependent on the particular MR technique employed [14].

Fat and water content

Bone marrow is rich in fat and water, which together contribute the bulk of the marrow signal seen on MRI. Alteration in the balance of lipid versus water in marrow is a principal factor affecting the signal intensity of marrow on MRI.

Lipid protons have short T1 relaxation times; therefore, yellow marrow has high signal intensity similar to that of subcutaneous fat in the T1-weighted spin-echo (SE) sequence. Red marrow, which has a higher water content than yellow marrow, has lower T1-weighted SE signal intensity than subcutaneous fat, but generally higher signal intensity than muscle and intervertebral discs. Most marrow lesions (benign or malignant) have a T1-weighted SE signal intensity similar to or lower than that of muscle, and are quite conspicuous against the background of high signal intensity yellow marrow (Fig. 3).

Using gradient echo chemical-shift imaging, the inherent differences in the resonance frequencies of water and lipid protons can be capitalized upon to evaluate the marrow for the presence of a tumor. When the appropriate echo time (e.g., TE=2.1 ms for a 1.5-T scanner) is used, the visualized signal intensity on the resultant opposed-phase image represents the difference between the signals from lipid and those from water; the result is a net cancellation of a portion of the overall signal from those voxels that contain both lipid and water.

Thus, the signal intensity from either red marrow or fatty marrow is decreased on opposed-phase imaging because both types of marrow contain fat and water (albeit in different proportions). In comparison, tumor deposits in marrow do not show signal loss on opposed-phase images because the vast majority of tumor deposits do not contain fat (Fig. 4).

Studies have suggested the potential of the chemical-shift MR technique as a complementary tool in predicting the likelihood that a marrow lesion is neoplastic. Disler et al. [15] studied the relative signal intensity ratios (defined as the ratio of signal intensity of a lesion versus control tissue on opposed-phase imaging divided by the corresponding ratio on in-phase imaging) of lesions in appendicular and pelvic bones. They found that the average relative signal intensity ratio for neoplastic lesions was 1.03, versus 0.61 for non-neoplastic lesions; using a relative signal intensity ratio higher than 0.81 resulted in a sensitivity and specificity of 95% for detection of a tumor. Zajick et al. [16] studied proportional change in signal intensity between in-phase and opposed-phase imaging of neoplastic and non-neoplastic lesions of the spine. They suggested that differences in signal intensity loss among normal, benign and malignant lesions were significant, with a decrease in signal intensity greater than 20% on opposed-phase imaging compared with in-phase imaging potentially being useful in distinguishing benign and malignant lesions. Erly et al. [17] similarly reported significant differences in signal intensity between benign and malignant spinal compression fractures on in-phase and opposed-phase imaging.

Another tool, the fat-suppression technique, facilitates detection of marrow lesions by suppressing signals from

Fig. 3 Spin-echo imaging of bone metastasis. a Axial T1-weighted MR image shows metastatic lesions from esophageal cancer in the intertrochanteric region of the femur with signal intensity lower than that of adjacent muscle. b Axial fat-suppressed T2-weighted MR image shows the signal intensity of the lesions as moderately higher than that of muscle
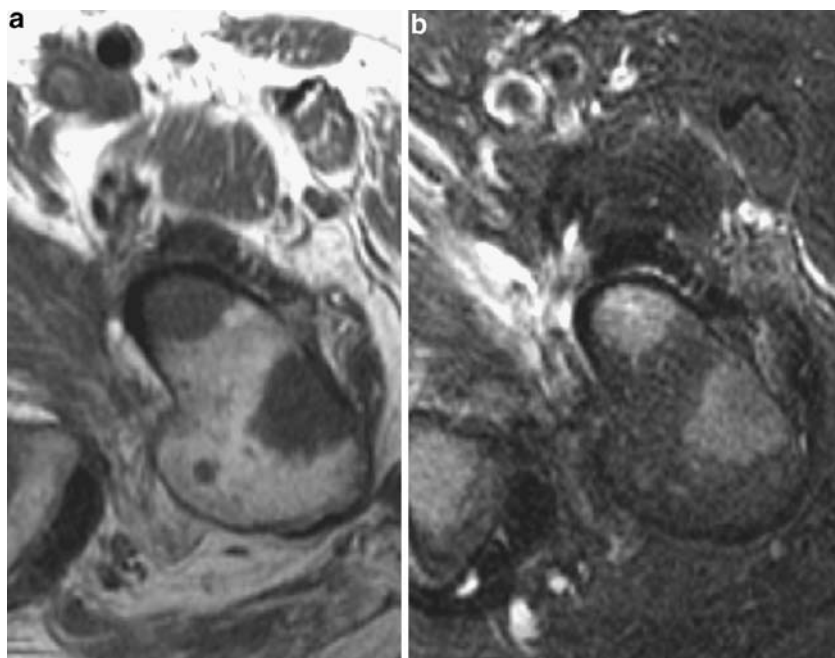
Fig. 4 Chemical-shift imaging of bone metastasis. **a** A tumor deposit (*T*) of renal cancer in the right pubic bone shows low signal intensity relative to normal bone marrow (*N*) on an axial in-phase gradient echo MR image (TE=4.2 ms at 1.5 T). **b** Normal marrow loses signal intensity on an opposed-phase gradient echo MR image (TE= 2.1 ms at 1.5 T) relative to an in-phase image, whereas the tumor deposit retains signal intensity. The signal intensity of the tumor deposit remains minimally lower than that of muscle on both images
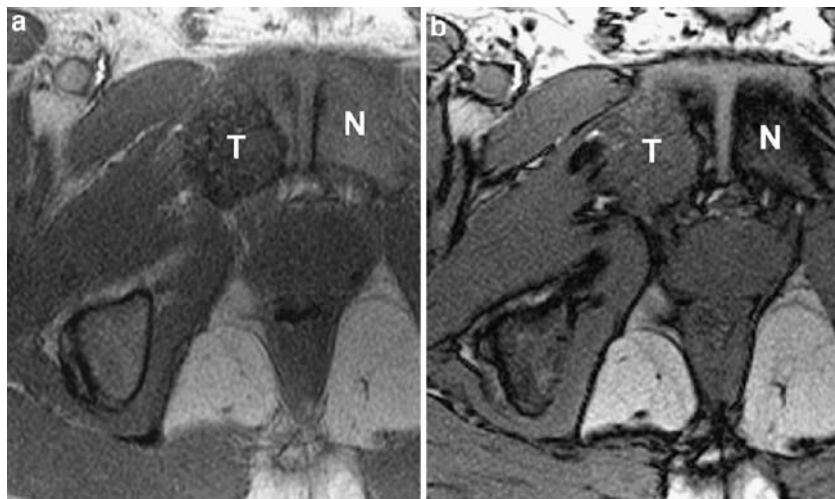
surrounding fat-containing marrow [18, 19]. A radiofrequency pulse of the same frequency as that of lipid is applied before the excitation pulse in order to selectively suppress the signals from lipid without affecting signals from other tissues—including those with a T1 relaxation time similar to that of lipid (such as some hematomas and contrast-enhanced tissues). Use of fat suppression is essential when using a fast (or turbo) SE T2-weighted sequence, as fatty marrow has moderately high signal that otherwise can mask the presence of concomitant tumor deposits on that sequence. However, this selective fat suppression technique is sensitive to susceptibility artifacts and requires excellent magnetic field homogeneity and a high magnetic field strength. In the presence of metal or air or when using a large field of view, the resultant fat suppression frequently is inhomogeneous; in fact, suppression of the water signal can inadvertently occur, thus obscuring pathologic conditions.

Alternatively, the short-tau inversion recovery (STIR) pulse sequence is less affected by inhomogeneous magnetic fields. In STIR, a 180° inversion pulse is delivered at the beginning of the sequence to invert the longitudinal magnetization; the differences in longitudinal magnetization of various tissues thus can be increased, improving T1-weighted contrast between tissues with relatively similar T1 relaxation times [20]. Selecting the inversion time (TI) such that the longitudinal magnetization of lipid has recovered to zero at the time of echo formation eliminates the signal from fatty tissue, thereby increasing the conspicuity of marrow abnormalities; at 1.5 T, use of a TI in the range of 150–170 ms will achieve this result. STIR is a highly sensitive technique in marrow lesion detection and is considered superior to T1-weighted SE in some studies [21]; however, the findings on STIR images often lack specificity because the STIR sequence suppresses signals from any other tissue that has a T1 relaxation time similar to that of fat. Additionally, in oncologic imaging, STIR may lead to overestimation of the extent of a marrow lesion due

to its demonstration of surrounding marrow edema pattern as high signal that may be similar to that of the lesion itself.

Diffusion-weighted imaging (DWI) can quantitatively assess the mobility of water molecules by allowing calculation of the apparent diffusion coefficient (ADC) [22]. Extracellular motion of free water is the main contributor to the ADC and signal loss in tissues [23, 24]. Therefore, the greater the extracellular motion of free water, the greater are the ADC value and the loss in signal intensity. As the restriction of water motion increases, the signal intensity increases. Tumor in marrow generally appears hyperintense on DWI due to restricted diffusion (Fig. 5).

Conflicting results have been reported for DWI in marrow imaging. In a study of benign and pathologic spinal compression fractures using SSFP DWI, Baur et al. [25] reported that all malignant compression fractures were hyperintense to normal marrow, whereas most benign compression fractures were hypointense to normal marrow. However, a subsequent study by Castillo et al. [26] showed no advantage of DWI in the detection and characterization of vertebral metastases compared with T1-weighted imaging; metastases were hypointense to normal marrow in 3 out of 5 patients with focal disease and 5 out of 10 patients with multiple lesions. In a study of lymphoma in the iliac bones by Yasumoto et al. [27], normal red marrow appeared hyperintense relative to lymphoma on DWI, with a sensitivity of 77% and specificity of 92.5%. Takahara et al. [28] suggested a feasible multiple thin-slice whole-body DWI technique and showed that MRI, like PET/CT, might potentially play a role in tumor survey and follow-up. However, more studies are needed to evaluate the clinical utility of DWI in marrow imaging.

Bony trabeculae

Trabecular bone produces little MR signal because it lacks mobile protons. However, trabeculae can decrease the signal

intensity of normal marrow by creating local magnetic field inhomogeneities at their innumerable interfaces with marrow. In SE sequences, the local field inhomogeneities caused by trabeculae are inapparent because their effects are largely canceled out by 180° refocusing pulses [12, 13, 29]. However, in gradient-echo imaging, which lacks a 180° refocusing pulse, the marrow in contact with trabecular bone loses signal as a result of T2* effects (spin dephasing due to local field inhomogeneities; Fig. 6). When lesions in the marrow destroy trabeculae, the signal from the affected marrow region is not decreased by such susceptibility effects [12, 29]; this change from normal can contribute to the detection of marrow lesions [12, 13].

Contrast enhancement

The commonly-employed gadolinium-based T1 MR contrast agents, as well as the T2 or T2* agents such as oxides, alter the local magnetic field by shortening relaxation times and thus selectively enhance the conspicuity of many lesions compared with neighboring tissues [30]. Gadolinium-DTPA has been the most widely used MR contrast agent in the clinical setting. Although enhancement of normal marrow is well shown on dynamic MRI after injection of gadolinium-DTPA, it is much less evident on routine T1-weighted SE MRI due to slower imaging times with resultant redistribution of contrast material [31, 32]. The enhancement of normal marrow is greatest in young patients and those with lower marrow fat content [31, 32]. Strong enhancement in both routine and dynamic contrast studies is usually seen in different pathological processes, including infection, inflammation, and tumor, and thus is a nonspecific finding. Fat suppression imaging increases lesion conspicuity and detection of enhancement (Fig. 7). T2 and T2* agents are still under investigation for their clinical utility; however, recent studies have shown that the different enhancement patterns seen with iron oxides, for example, help in detecting marrow lesions and distinguishing red marrow from neoplastic marrow by providing high marrow-to-tumor contrast [33, 34]. Given the large number
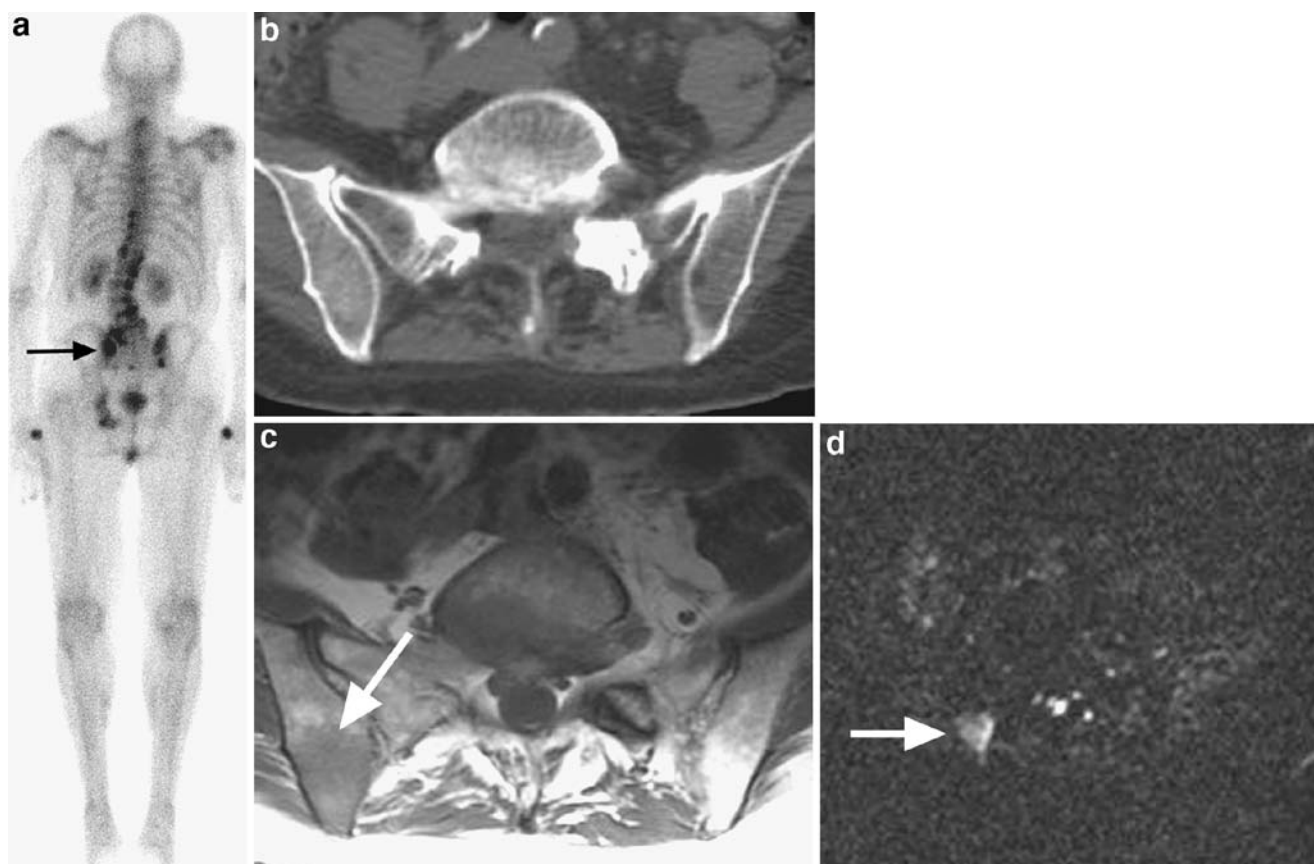
Fig. 5 Diffusion-weighted imaging of blastic bone metastasis from prostate cancer. a Bone scan (posterior view) shows intense uptake in a right iliac lesion (arrow) near the sacroiliac joint, as well as in several other lesions in the spine and bony pelvis. b On a CT scan, the right ilium in the corresponding location appears mildly sclerotic compared with the left ilium, without gross trabecular or cortical destruction. c Axial T1-weighted MR image shows low signal intensity lesion (arrow) in the corresponding location in the right ilium. d Axial MR diffusion-weighted image (b value=10,00 s/mm²) shows the right iliac lesion as a high-signal focus (arrow). (Case courtesy of Eric Lis, MD, Memorial Sloan-Kettering Cancer Center, New York, NY, USA)

Fig. 6 Effect of bony trabeculae on MR signal intensity. **a** Coronal T1-weighted SE MR image shows high signal intensity throughout visualized bone marrow of proximal femur. Coronal gradient-echo MR images obtained with **b** TE= 5.1 ms and **c** TE=12.6 ms reveal greater degrees of signal loss in marrow with increasing TEs, at least partly due to T2* effects from local field inhomogeneities caused by interfaces between bony trabeculae and marrow
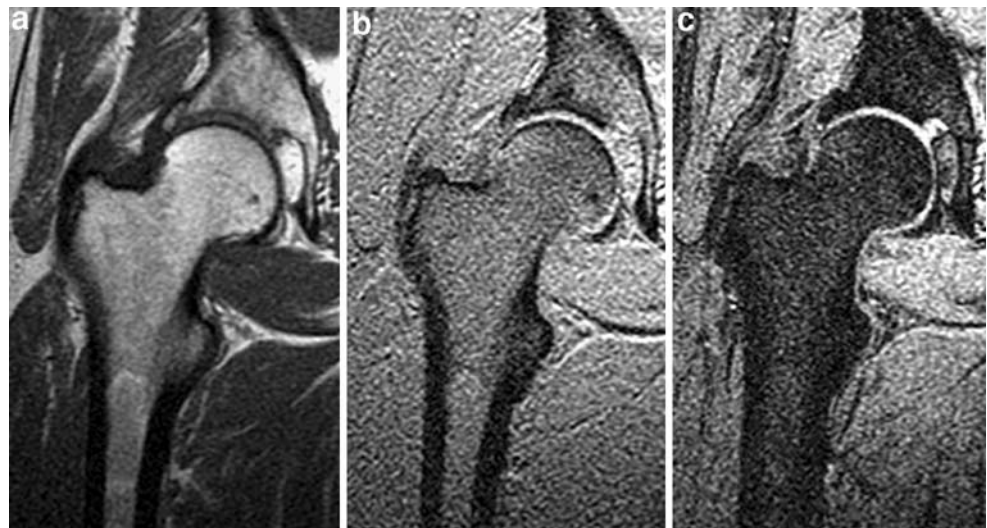
of MR contrast agents under development, clinical application of these agents likely will increase in the future; understanding the mechanism of action of these agents will be necessary to optimize the technical parameters used.

Distinguishing normal and abnormal marrow on MRI: normal variations in marrow, including marrow heterogeneity

The proportions of adipocytes and hematopoietic cells in marrow can change focally or diffusely, resulting in a normal heterogeneity of the marrow on MRI (Fig. 8) that may be confused with marrow lesions. The signal intensity,

morphology, and distribution of marrow can help to distinguish such normal variations from marrow lesions.

Islands of yellow marrow are readily recognizable by their signal intensity, which is similar to that of subcutaneous fat in all sequences (Fig. 8). Islands of red marrow remain intermediate in signal intensity on T2-weighted images due to increased hematopoietic cellularity and water content; their signal intensity on T1-weighted images is lower than that of fat but often higher than that of muscle (in contrast to tumor deposits, which are generally isointense or hypointense to muscle; Fig. 3a)—a finding that the authors find especially useful. Foci of red marrow also can often be recognized by their poorly defined, feathery margins that interdigitate with fatty marrow (Fig. 9a), as well as by a
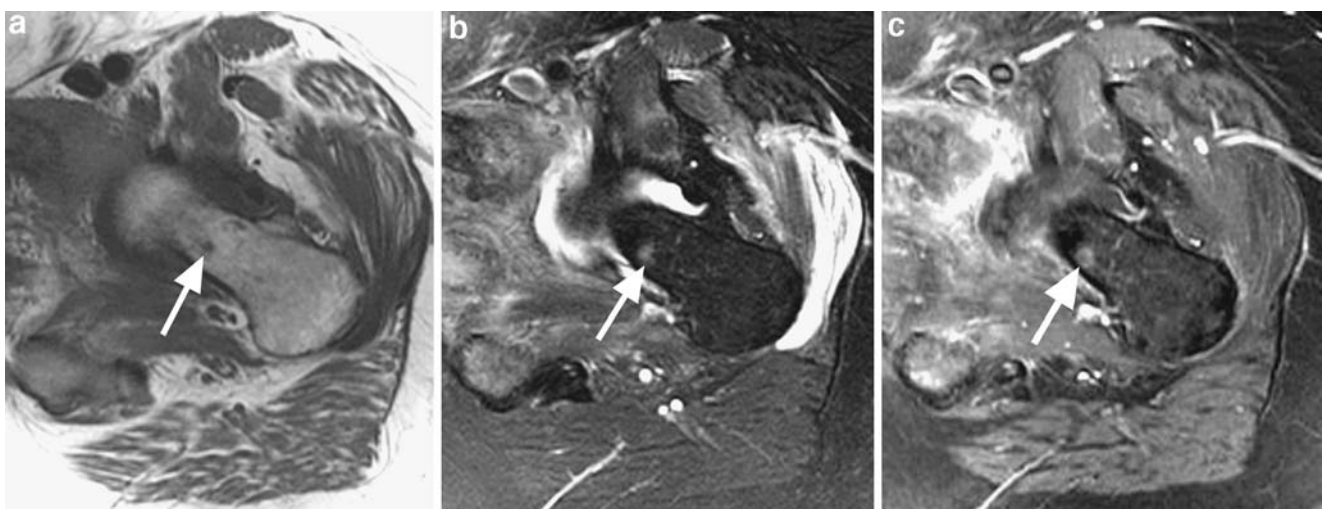
Fig. 7 Enhancement of bone metastasis from bladder cancer. **a** Axial T1-weighted and **b** fat-suppressed T2-weighted MR images show a small, indistinct lesion in the left femoral neck (*arrow*). (Patient moved slightly between image series, accounting for slight misregis-

tration between images.) **c** Axial contrast-enhanced fat-suppressed T1-weighted MR image shows rim enhancement of the lesion, increasing lesion conspicuity and implicating a malignant etiology of the lesion, despite its small size
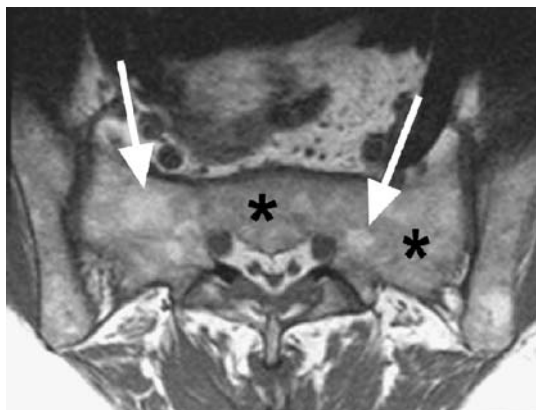
Fig. 8 Normal heterogeneity of marrow. Islands of fatty marrow (*arrows*) are evident within a background of red marrow (*asterisks*) in sacrum. Pelvic marrow is often heterogeneous, reflecting the transitional location of the pelvis between (axial, red-marrow-containing) spine and (peripheral, yellow-marrow-containing) femurs

symmetrical distribution; in distinction, marrow metastases tend to be more rounded and sharply defined (Fig. 3a).

Focal or diffuse red marrow generally has relatively low signal intensity on fat-suppressed T2-weighted SE images (Fig. 9b,d). In adults, red marrow deposits generally would not be present in epiphyses or apophyses (Fig. 9c) unless severe reconversion was already present throughout the diaphyses and metaphyses of the affected bone. In the

setting of advanced marrow reconversion, the borders of regions of red marrow become more sharply defined and their signals further decrease on T1-weighted SE imaging; limited contrast enhancement in red marrow regions on T1-weighted SE imaging is another finding that suggests a benign nature [11, 35].

Summary

Magnetic resonance imaging is an excellent noninvasive modality for evaluating bone marrow and detecting marrow lesions, as it provides information at the level of cellular and chemical composition, in addition to gross morphologic data. Knowledge of normal marrow components and composition and their variation, as well as of factors that alter MR signal intensity, is important for optimal interpretation of MR images. The signal intensity, morphology, and location of marrow findings on MRI can be used to provide more accurate diagnoses, to guide treatment, and to follow therapy-related changes. Various MR imaging techniques are available to accentuate the different chemical and cellular compositions of normal marrow and marrow diseases. Although MRI is more sensitive than specific in detecting marrow changes, integrating all the clinical and radiologic

Fig. 9 Morphology and distribution of red marrow. **a** Coronal T1-weighted SE MR image shows red marrow as having signal intensity slightly lower than that of fat, but a considerably higher signal than that of muscle. The morphology of focal regions of red marrow often is feathery (*arrow*). **b** Coronal fat-suppressed T2-weighted MR image of the same patient as in **a** shows low to intermediate signal intensity of red marrow (*arrow*), only minimally higher than that of muscle. **c** T1-weighted SE MR image of a different patient shows a more diffuse distribution of red marrow in the proximal femur, but its signal intensity remains considerably higher than that of muscle. **d** Coronal fat-suppressed T2-weighted MR image in the same patient as in **c** shows the diffuse low-signal intensity of red marrow, which would be unusual in marrow that contains a tumor (unless a radiograph or CT scan showed dense sclerosis in the same region)

data can result in more useful interpretations. The MRI evaluation of tumor and post-treatment changes in marrow, as well as some promising complementary MR techniques under evaluation, will be discussed in part 2 of this article.

References

1. Steiner RM, Mitchell DG, Rao VM, Schweitzer ME. Magnetic resonance imaging of diffuse bone marrow disease. Radiol Clin North Am 1993; 31: 383–409.
2. Snyder WS, Cook MJ, Nasset ES, Karhausen LR, Howells CP, Tipton IH. International Commission on Radiological Protection. Report of the task group on reference man. Oxford: Pergamon; 1975. pp. 79–98.
3. Vande Berg BC, Malghem J, Lecouvet FE, Maldague B. Magnetic resonance imaging of the normal bone marrow. Skeletal Radiol 1998; 27: 471–483.
4. Piney A. The anatomy of the bone marrow: with special reference to the distribution of the red marrow. BMJ 1922; 28: 792–795.
5. Moore SG, Dawson KL. Red and yellow marrow in the femur: age-related changes in appearance at MR imaging. Radiology 1990; 175: 219–223.
6. Ricci C, Cova M, Kang YS, et al. Normal age-related patterns of cellular and fatty bone marrow distribution in the axial skeleton: MR imaging study. Radiology 1990; 177: 83–88.
7. Hartsock RJ, Smith EB, Petty CS. Normal variations with aging of the amount of hematopoietic tissue in bone marrow from the anterior iliac crest. A study made from 177 cases of sudden death examined by necropsy. Am J Clin Pathol 1965; 43: 326–331.
8. Shellock FG, Morris E, Deutsch AL, Mink JH, Kerr R, Boden SD. Hematopoietic bone marrow hyperplasia: high prevalence on MR images of the knee in asymptomatic marathon runners. Am J Roentgenol 1992; 158: 335–338.
9. Poulton TB, Murphy WD, Duerk JL, Chapek CC, Feiglin DH. Bone marrow reconversion in adults who are smokers: MR imaging findings. Am J Roentgenol 1993; 161: 1217–1221.
10. Stabler A, Doma AB, Baur A, Kruger A, Reiser MF. Reactive bone marrow changes in infectious spondylitis: quantitative assessment with MR imaging. Radiology 2000; 217: 863–868.
11. Vande Berg BC, Lecouvet FE, Galant C, Maldague BE, Malghem J. Normal variants and frequent marrow alterations that simulate bone marrow lesions at MR imaging. Radiol Clin North Am 2005; 43: 761–770.
12. Vanel D, Dromain C, Tardivon A. MRI of bone marrow disorders. Eur Radiol 2000; 10: 224–229.
13. Vanel D, Bittoun J, Tardivon A. MRI of bone metastases. Eur Radiol 1998; 8: 1345–1351.
14. Panicek DM, Schwartz LH. MR imaging of bone marrow in patients with musculoskeletal tumors. Sarcoma 1999; 3: 37–41.
15. Disler DG, McCauley TR, Ratner LM, Kesack CD, Cooper JA. In-phase and out-of-phase MR imaging of bone marrow: prediction of neoplasia based on the detection of coexistent fat and water. Am J Roentgenol 1997; 169: 1439–1447.
16. Zajick DC Jr, Morrison WB, Schweitzer ME, Parellada JA, Carrino JA. Benign and malignant processes: normal values and differentiation with chemical shift MR imaging in vertebral marrow. Radiology 2005; 237: 590–596.
17. Erly WK, Oh ES, Outwater EK. The utility of in-phase/opposed-phase imaging in differentiating malignancy from acute benign compression fractures of the spine. Am J Neuroradiol 2006; 27: 1183–1188.
18. Keller PJ, Hunter WW Jr, Schmalbrock P. Multisection fat-water imaging with chemical shift selective presaturation. Radiology 1987; 164: 539–541.
19. Mitchell DG, Vinitski S, Rifkin MD, Burk DL Jr. Sampling bandwidth and fat suppression: effects on long TR/TE MR imaging of the abdomen and pelvis at 1.5 T. Am J Roentgenol 1989; 153: 419–425.
20. Bushong S. Magnetic resonance imaging: physical and biological principles. 3rd edn. St. Louis: Mosby; 2003.
21. Mirowitz SA, Apicella P, Reinus WR, Hammerman AM. MR imaging of bone marrow lesions: relative conspicuousness on T1-weighted, fat-suppressed T2-weighted, and STIR images. Am J Roentgenol 1994; 162: 215–221.
22. Baur A, Reiser MF. Diffusion-weighted imaging of the musculo-skeletal system in humans. Skeletal Radiol 2000; 29: 555–562.
23. Baur A, Stabler A, Huber A, Reiser M. Diffusion-weighted magnetic resonance imaging of spinal bone marrow. Semin Musculoskelet Radiol 2001; 5: 35–42.
24. Plecha DM. Imaging of bone marrow disease in the spine. Semin Musculoskelet Radiol 2000; 4: 321–327.
25. Baur A, Stabler A, Bruning R, et al. Diffusion-weighted MR imaging of bone marrow: differentiation of benign versus pathologic compression fractures. Radiology 1998; 207: 349–356.
26. Castillo M, Arbelaez A, Smith JK, Fisher LL. Diffusion-weighted MR imaging offers no advantage over routine noncontrast MR imaging in the detection of vertebral metastases. AJNR Am J Neuroradiol 2000; 21: 948–953.
27. Yasumoto M, Nonomura Y, Yoshimura R, et al. MR detection of iliac bone marrow involvement by malignant lymphoma with various MR sequences including diffusion-weighted echo-planar imaging. Skeletal Radiol 2002; 31: 263–269.
28. Takahara T, Imai Y, Yamashita T, Yasuda S, Nasu S, Van Cauteren M. Diffusion weighted whole body imaging with background body signal suppression (DWIBS): technical improvement using free breathing, STIR and high resolution 3D display. Radiat Med 2004; 22: 275–282.
29. Sebag GH, Moore SG. Effect of trabecular bone on the appearance of marrow in gradient-echo imaging of the appendicular skeleton. Radiology 1990; 174: 855–859.
30. Hendrick RE, Haacke EM. Basic physics of MR contrast agents and maximization of image contrast. J Magn Reson Imaging 1993; 3: 137–148.
31. Montazel JL, Divine M, Lepage E, Kobeiter H, Breil S, Rahmouni A. Normal spinal bone marrow in adults: dynamic gadolinium-enhanced MR imaging. Radiology 2003; 229: 703–709.
32. Chen W, Shih T, Chen R, et al. Vertebral bone marrow perfusion evaluated with dynamic contrast-enhanced MR imaging: significance of aging and sex. Radiology 2001; 220: 213–218.
33. Daldrup-Link HE, Rummeny EJ, Ihssen B, Kienast J, Link TM. Iron-oxide-enhanced MR imaging of bone marrow in patients with non-Hodgkin's lymphoma: differentiation between tumor infiltration and hypercellular bone marrow. Eur Radiol 2002; 12: 1557–1566.
34. Metz S, Lohr S, Settles M, et al. Ferumoxtran-10-enhanced MR imaging of the bone marrow before and after conditioning therapy in patients with non-Hodgkin lymphomas. Eur Radiol 2006;16:598–607.
35. Levine CD, Schweitzer ME, Ehrlich SM. Pelvic marrow in adults. Skeletal Radiol 1994; 23: 343–347.